J Biol Inorg Chem (2006) 11: 119–127
DOI 10.1007/s00775-005-0054-9

ORIGINAL ARTICLE

Smilja Todorovic · Christiane Jung · Peter Hildebrandt
Daniel H. Murgida

Conformational transitions and redox potential shifts of cytochrome P450 induced by immobilization

Received: 6 April 2005 / Accepted: 26 October 2005 / Published online: 3 December 2005

Abstract Cytochrome P450 (P450) from *Pseudomonas putida* was immobilized on Ag electrodes coated with self-assembled monolayers (SAMs) via electrostatic and hydrophobic interactions as well as by covalent cross-linking. The redox and conformational equilibria of the immobilized protein were studied by potential-dependent surface-enhanced resonance Raman spectroscopy. All immobilization conditions lead to the formation of the cytochrome P420 (P420) form of the enzyme. The redox potential of the electrostatically adsorbed P420 is significantly more positive than in solution and shows a steady downshift upon shortening of the length of the carboxyl-terminated SAMs, i.e., upon increasing the strength of the local electric field. Thus, two opposing effects modulate the redox potential of the adsorbed enzyme. First, the increased hydrophobicity of the heme environment brought about by immobilization on the SAM tends to upshift the redox potential by stabilizing the formally neutral ferrous form. Second, increasing electric fields tend to stabilize the positively charged ferric form, producing the opposite effect. The results provide insight into the parameters that control the structure and redox properties of heme proteins and contribute to the understanding of the apparently anomalous behavior of P450 enzymes in bioelectronic devices.

S. Todorovic · P. Hildebrandt · D. H. Murgida
Instituto de Tecnologia Química e Biológica,
Universidade Nova de Lisboa, Apartado 127,
2781-901 Oeiras, Portugal

C. Jung
Max-Delbrück-Centrum für Molekulare Medizin,
Robert-Rössle-Strasse 10, 13125 Berlin, Germany

P. Hildebrandt · D. H. Murgida (✉)
Institut für Chemie, Max-Volmer-Laboratorium
für Biophysikalische Chemie, Sekr. PC14,
Technische Universität Berlin, Strasse des 17. Juni 135,
10623 Berlin, Germany
E-mail: dh.murgida@tu-berlin.de
Tel.: +49-30-31426500
Fax: +49-30-31421122

Keywords Cytochrome P450 · Enzyme immobilization · Redox potential · Electrostatic interactions · Surface-enhanced resonance Raman spectroscopy

Introduction

Cytochromes P450 (P450) represent a large family of heme-containing enzymes, found in all types of living organisms. The P450 isozymes catalyze a variety of biological oxidation reactions in the degradation of exogenous compounds as well as in biosynthesis. The P450 family includes soluble and membrane-bound proteins with quite different overall structures. Common features of all P450 isozymes, however, are the unique ligation pattern of the redox site, in which a thiolate is coordinated to the heme iron, and the mechanism of the reaction cycle which involves the activation of molecular oxygen as the key step. The substrate binds in proximity to the heme to allow for the reaction with activated oxygen. The unique structure of the substrate binding pocket ensures substrate selectivity, product selectivity, and regioselectivity of the enzymatic reaction, which are very high for many isozymes [1–7].

Owing to the large variety of oxygenic reactions that different P450s perform with high efficiency and selectivity, this superfamily constitutes an enormous source of potential biocatalysts for chemical synthesis, and has indeed stimulated considerable research activities in this field [8–11].

A widely used approach for fabricating P450-based biocatalytic devices consists in immobilizing the enzymes on electrodes that may serve as a controllable electron source to drive the reaction cycle [12–20]. Previous studies have in fact shown that P450 can be immobilized in an electroactive form, although the reported redox potentials span a range of more than 0.15 V in the various immobilized systems and, moreover, differ substantially from that of P450 in solution [13–20]. The origin of these shifts of potentials is yet

unclear and structural changes of the protein caused by the immobilization cannot be ruled out. So far, immobilized P450 has not been monitored in situ by spectroscopic techniques that provide insight into the active-site structure.

Such information can be provided by resonance Raman (RR) spectroscopic techniques that selectively probe the vibrational bands of the heme group upon excitation in resonance with its electronic transition. When heme proteins are in close proximity to an Ag surface, the RR bands are further enhanced by several orders of magnitude (surface-enhanced RR, SERR) such that it is possible to probe the redox site solely of the immobilized proteins. This technique has been successfully applied to electron-transferring cytochromes using Ag electrodes that were coated with self-assembled monolayers (SAMs) with various head groups [21]. In this way, direct contact of the protein with the metal surface, which may cause severe perturbations of the native structure, is avoided. Up to now, this approach has not yet been employed to P450 adsorbed on coated electrodes, but it has been shown that preadsorption of organic anions on Ag colloids may provide a "biocompatible" surface that largely reduces the protein structural changes of the bound enzyme [22–24].

In this work, we have investigated the interfacial redox processes of the soluble P450 from *Pseudomonas putida*, which is the best characterized member of the P450 superfamily. For this P450 isozyme, crystal structures have been determined for various states and the reaction cycle has been analyzed in great detail by a variety physicochemical techniques [23, 25–35]. Thus, the large body of available structural, thermodynamic, kinetic, and spectroscopic data serves as a reference for the present study in which P450 is immobilized on SAM-coated Ag electrodes. SAMs were prepared from alkyl thiols of different chain lengths and tail groups that allow for different modes of immobilization. We have analyzed the adsorption-induced and potential-dependent structural changes of the heme site by SERR spectroscopy, and determined the redox potentials of the enzyme immobilized under different conditions.

Materials and methods

Protein isolation and purification and chemicals

P450 from *P. putida* was overexpressed in *Escherichia coli* and purified as described elsewhere [36]. Camphor-bound P450 was prepared as previously described [37].

Mercaptoacetic acid (C_2), 3-mercaptopropionic acid (C_3), 11-mercaptoundecanoic acid (C_{11}), 16-mercapto-hexadecanoic acid (C_{16}), ethanethiol, pentanethiol, 1-decanethiol, and 1-ethyl-3-(3-dimethylaminopropyl)-carbodiimide (EDC) were purchased from Sigma and were used without further purification. 5-Carboxy-1-pentanethiol (C_6), 6-aminohexanethiol, and 11-aminoundecanethiol were purchased from Dojindo Laboratories.

Electrode modification and protein immobilization

Protocols for the preparation of the SERR-active Ag surfaces as well as subsequent coating of the electrode (geometrical surface approximately 0.75 cm^2) with SAMs of various carboxylate-, amino-, and methyl-terminated alkylthiols followed published procedures [38].

For electrostatic adsorption, the SAM-coated electrodes were immersed into a 0.1 μM solution of P450 (12.5 mM potassium phosphate, 12.5 mM K_2SO_4) adjusted to pH 7.5 and left to equilibrate for 45 min.

Covalent cross-linking was accomplished with EDC to form amide bonds between the carboxyl groups of the SAMs and basic amino acid residues on the protein surface. The reaction conditions were optimized by varying the concentration of EDC (0.1–5 mM), incubation times (1–5 min), and potential of the electrode (−0.35 to +0.15 V) during incubation. After completion of the reaction the electrodes were rinsed and immersed in the electrochemical cell containing buffers of different pH values (6.5–7.5).

RR and SERR spectroscopy

RR and SERR spectra were measured with the 413-nm line of a krypton ion laser (Coherent Innova 302), using a confocal spectrograph (Jobin Yvon, XY) equipped with a grating of 1,800 lines mm^{-1} and a liquid nitrogen cooled back-illuminated CCD camera. The spectral resolution was approximately 2 cm^{-1} and the increment per data point approximately 0.47 cm^{-1}.

RR spectra were obtained from 10 μM aqueous solutions of P450 (20 mM potassium phosphate buffer, pH 7.5), contained in a rotating cuvette. Reduction was achieved by addition of dithionite. The acquisition time for the spectra was approximately 40 s, using a laser power of 1.2 mW.

In SERR spectroscopic experiments, the laser beam was focused onto the surface of a home-built rotating electrode with a power of approximately 3.5 mW at the sample. A detailed description of the electrochemical setup is given elsewhere [38]. The spectral accumulation time was typically 60 s.

All experiments were carried out with buffered solutions (12.5 mM potassium phosphate, 12.5 mM K_2SO_4) adjusted to pH 7.5, unless stated otherwise. Prior to and during the SERR experiments, the electrochemical cell was purged by a continuous stream of catalytically purified oxygen-free argon gas. All the potentials cited in this work refer to the normal hydrogen electrode.

After background subtraction the spectra were submitted to component analysis in which the spectra of the individual species were fitted to the measured spectra [39].

Results and discussion

Structure of P450 immobilized on negatively charged surfaces

Substrate-free P450 was electrostatically immobilized on Ag electrodes coated with SAMs of ω-carboxyl alkanethiols of different chain lengths, containing between 1 and 15 methylene groups. The adsorption of the protein to the negatively charged surfaces was monitored by SERR spectroscopy under conditions that allow for the sensitive detection of the heme groups solely of the adsorbed species without interference of protein molecules in the bulk solution.

At all monolayers, the adsorbed P450 gives rise to qualitatively the same SERR spectra although the overall intensity displays the expected decrease with increasing chain length of the SAM. Upon switching the electrode potential from −0.4 to +0.34 V, the oxidation-state-sensitive marker bands ν_2, ν_3, and ν_4 of the heme undergo frequency upshifts of approximately 10 cm^{-1}, indicating that the adsorbed heme protein is redox-active (Fig. 1, spectra b, c) [26].

A similar immobilization strategy has been successfully applied to different heme proteins, e.g., cytochrome *c* (cyt-*c*) [21] and cytochrome c_3 (cyt-c_3) [40, 41]. Unlike P450, these proteins possess well-defined positively charged binding domains around the partially exposed heme redox center that allow for a largely uniform orientation of the protein in electrostatic complexes and guarantee good electronic communication with the electrode. In the case of P450, the heme group is buried in the protein matrix and no extended cationic patches can be identified on the protein surface by visual inspection of the crystal structure (Protein Data Bank entry 1PHC). However, a few positively charged residues on the proximal side of the protein (around Arg112) have been shown to be involved in electrostatic interactions with putidaredoxin such that the closest approach of the two redox centers is approximately 8 Å [31, 33, 42]. Although the present study does not provide direct information on the orientation of the adsorbed species, it is very likely that the same residues are involved in the electrostatic immobilization to negatively charged SAM-coated electrodes.

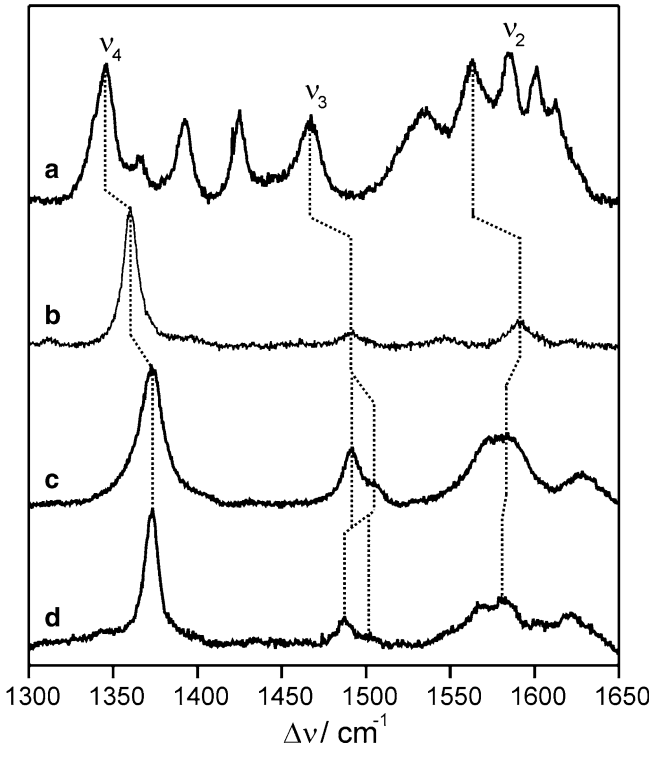

Fig. 1 Surface-enhanced resonance Raman (*SERR*) and resonance Raman (*RR*) spectra of cytochrome P450 on a 11-mercaptoundecanoic acid (C_{11}) self-assembled monolayer (*SAM*) coated electrode and in solution, respectively. *a* RR, dithionite reduced form. *b* SERR, ferrous form at −0.40 V. *c* SERR, ferric form at 0.34 V. *d* RR, ferric form

A comparison of the SERR spectra of the immobilized P450 recorded at negative potentials (below −0.1 V) with the RR spectrum of the fully reduced protein in solution (Fig. 1, spectra a, b, Table 1) shows that electrostatic immobilization induces substantial alterations of the protein structure on the level of the heme pocket.

The reduced form of substrate-free P450 possesses a five-coordinated high-spin (5cHS) heme in which the axial ligand is a thiolate (Cys 357) [30]. Owing to the electron density push from the negatively charged sulfur ligand to the iron, a stronger iron-π back-donation to the porphyrin π system is induced, thereby specifically weakening the C–N bonds. This effect is reflected by an unusually low frequency of the ν_4 mode of ferrous P450 (approximately 1,350 cm^{-1}) [25, 26, 34]. In the SERR spectra, however, the ν_4 frequency is found at 1,361 cm^{-1}, which is as high as in "normal" ferrous hemes and thus indicates the replacement of the thiolate by a less-electron-donating ligand. Furthermore, the positions and relative intensities of the ν_2, ν_3, and ν_4 marker bands of the adsorbed enzyme are consistent with a six-coordinated low-spin (6cLS) configuration of a ferrous heme [43]. Thus, the SERR spectrum is closely related to the RR spectrum of the ferrous pressure-induced cytochrome P420 (P420) form of the enzyme as reported by Wells et al. [34]. In this largely inactive state, which is common to all members of the P450 superfamily, the protein undergoes a structural change that involves a modification of the ligation pattern including the removal or the protonation of the thiolate ligand [27, 34, 35, 44, 45].

A comparison of the SERR spectrum of the adsorbed enzyme in the oxidized (above +0.1 V) state with the RR spectrum of P450 in solution shows less pronounced yet distinct differences (Fig. 1, spectra c, d). Whereas the marker bands in the RR spectrum of the substrate-free ferric P450 reflect the 6cLS configuration of the heme

Table 1 Positions v_i and intensities I (v_i) (arbitrary units) of the v_2, v_3, and v_4 bands of the six-coordinated low-spin (*6cLS*) and five-coordinated high-spin (*5cHS*) species, detected by surface-enhanced resonance Raman spectroscopy upon formation of cytochrome P420 (*P420*) on sulfate-coated electrode in this work, and based on resonance Raman spectra reported by Wells et al. [34]

	6cLS				5cHS			
	Reduced		Oxidized		Reduced		Oxidized	
v_4(cm^{-1})	1360.6	1,361[a]	1373.6	1,374[a]	1357.9		1371.6	
I (v_4)	1		1		1		1	
v_3(cm^{-1})	1491.9	1,493[a]	1503.9	1,503[a]	1470.1	1,470[a]	1491.2	1,491[a]
I (v_3)	0.112		0.154		0.120		0.595	
v_2(cm^{-1})	1,584	1,583[a]	1,590	1,588[a]	1,562	1,560[a]	1,570	1,572[a]
I (v_2)	0.198		0.287		0.05		0.310	

[a]Based on resonance Raman spectra reported by Wells et al. [34]

with a thiolate and a water molecule serving as axial ligands, the SERR spectra of the adsorbed oxidized protein suggest an equilibrium between at least two different heme structures. This is particularly reflected by the v_3 region, where two distinct bands can be identified at 1,504 and 1,491 cm^{-1}, as well as by the substantial broadening of the v_4 band envelope. The band-fitting analysis indicates that all SERR spectra of the ferric adsorbed protein can be consistently simulated with two components, corresponding to a 6cLS and a 5cHS heme. Again, we note far-reaching similarities with the RR spectra of ferric P420 reported by Wells et al. [34] which also display the characteristic signature of a 6cLS/5cHS coordination equilibrium.

Upon substrate binding, ferric P450 is also transformed into the 5cHS configuration and the spectral differences between P450 and P420 are less pronounced in the ferric state [25, 32, 34]. However, immobilization of the substrate-free and the substrate-bound P450 yielded essentially the same SERR spectra with the same 5cHS/6cLS distribution. Furthermore, formation of the adsorbed ferric 5cHS and 6cLS species from the ferrous P420 is reversible (vide supra) in several oxidation–reduction cycles. Thus, we conclude that in the ferrous and the ferric state the enzyme exists in the P420 form, generated upon binding of P450 to the SAM-coated electrode.

The main difference between the SERR spectra of the adsorbed P420 and the RR spectra reported for P420 in solution [34] refers to the coordination equilibrium. In contrast to P420 in solution, no ferrous 5cHS species can be detected in the adsorbed state. This discrepancy can be understood by taking into account that the P420 state may not be characterized by a uniform and well-defined protein structure [45]. The transformation from P450 to P420 can be caused by changing a variety of parameters, including temperature, pH, ionic strength, detergent, and solvent composition [28, 29, 34, 35, 44, 46–51]. Although each of these P420 forms lacks the strong electron-donating capacity of a thiolate ligand, structural details of their heme pockets may be different. In the immobilized state, the crucial parameter that is likely to cause the conversion from P450 to P420 is the electric field strength, which results from the (distance-dependent) interfacial potential drop across the SAM and the local distribution of charges on the SAM surface [21, 38, 52, 53].

The putative interaction domain of P450 for binding to the anionic surface lies directly above the cysteine axial ligand on the proximal side [33]. Thus, electrostatic interactions through this region can be expected to affect the heme coordination as is observed even for the P450–putidaredoxin complex [31]. In this case, the native thiolate ligand remains preserved but the 5cHS/6cLS equilibrium of the ferric substrate-bound P450 is shifted towards the 6cLS configuration.

The strength of the interfacial electric fields at SAM-coated Ag electrodes has been found to be sufficient to destabilize even the compact heme pocket structure of the electron-transferring protein cyt-*c* [21, 38]. Specifically, the coordinative Fe–Met bond is weakened such that in the adsorbed state native cyt-*c* (B1 state) is in equilibrium with a new state (B2) that lacks the Met ligand but retains the native secondary structure. Upon increasing the electric field strength the B2-to-B1 equilibrium ratio increases such that at short chain lengths (high electric fields) B2 prevails, whereas at the longest chain lengths the immobilized cyt-*c* remains exclusively in the native B1 state. Since there is no indication for the native P450 state even at the longest (C_{16}) monolayer, we conclude that the conversion of the immobilized P450 to P420 occurs even at relatively weak electric fields.

The interfacial electric field does not only induce the formation of P420, but also appears to weaken the ligand field in the immobilized P420 itself since it forms a 5cHS/6cLS equilibrium in the ferric state. In contrast, the ferrous P420 exclusively exists in the 6cLS configuration regardless of the SAM chain length. These findings imply that the two axial ligands form stronger coordinative bonds in the reduced than in the oxidized heme, which is consistent with the coordination by a histidine and either a water or a protonated cysteine [54, 55]. The situation is different when the carboxyl-terminated thiol monolayers are replaced by divalent anions (sulfate) that are specifically adsorbed on the bare Ag electrode. Under these conditions the electric field strength is increased and then also the ferrous state of

the immobilized P420 displays marker bands that are characteristic of a 5cHS configuration, such as a band at 1,470 cm^{-1} (ν_3 mode) and a dominant feature at 1,358 cm^{-1} (ν_4 mode) (Fig. 2, spectra a).

At all potentials the SERR spectra of P420 immobilized on sulfate-coated electrodes can be quantitatively simulated on the basis of the same components determined for SAM coatings, i.e., $6cLS^{red}$, $6cLS^{ox}$, and $5cHS^{ox}$, plus an additional component spectrum of a ferrous 5cHS heme, $5cHS^{red}$ (Fig. 2, Table 1).

Further immobilization strategies

In order to avoid or, at least, to reduce the conversion of P450 to P420 induced by the electric field, we employed various immobilization strategies. The electric field strength experienced by the heme site is controlled by the potential drop across the SAM and the charge distribution in the SAM/solution interface [21, 38] and thus may be lowered either by reducing the charge density at the binding site for the protein or by increasing the SAM thickness. The latter possibility was not considered to be a promising approach. Namely, the distance-dependent decrease of the SERR effect impairs the spectroscopic analysis of the protein bound to SAMs that contain distinctly more than 15 methylene groups, which would, however, be required for a significant reduction of the field strength. Our studies, therefore, focused on the modification of the local charge distribution in the SAM/protein interface. Increasing the ionic strength from 60 to 160 mM, which compresses the electrical double layer and thus lowers the field strength at the heme pocket, did not affect the P420 formation. Higher ionic strengths caused desorption of the protein from the SAM surface such that a SERR spectroscopic analysis was not possible.

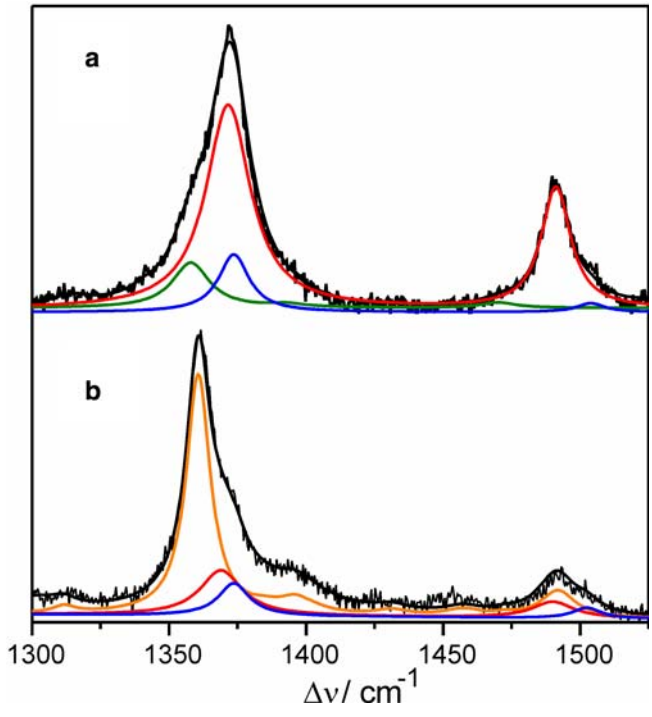

Fig. 2 SERR experimental and component spectra of cytochrome P420 (*P420*) immobilized on two different coatings. *a* P420 on a sulfate-coated electrode, measured at −0.15 V. *b* P420 on a C_{11} SAM coated electrode measured at 0.10 V. *Black lines* experimental and fitted spectral, *red lines* oxidized five-coordinated high-spin ($5cHS^{ox}$) component, *green lines* reduced five-coordinated high-spin component. *Blue lines* oxidized six-coordinated low-spin ($6cLS^{ox}$) component, *orange lines* reduced six-coordinated low-spin ($6cLS^{red}$ component)

In an attempt to reduce the charge density on the SAM surface, mixed monolayers of ω-carboxyl-alkanethiols and methyl-terminated alkanethiols were formed with molar ratios ranging from 1:10 to 1:1. The SERR spectra did not provide any indication for the native enzyme in any of the cases, suggesting that the dilution effect is compensated by a decrease of the pK_a of the carboxylate groups such that the overall surface charge density remains largely unchanged. Reducing the charge density by decreasing the pH from 7.5 to 6.5 did not produce any significant effect either. Even lower pH values induce protein desorption. Covalent cross-linking via EDC either to carboxylate-terminated or to amino-terminated SAMs and subsequent lowering of the pH was also unsuccessful in preserving the native P450 form. Noncovalent immobilization of the enzyme to methyl- and amino-terminated monolayers also yielded the inactive P420 state but the surface concentration of the protein was substantially lower than on anionic coatings as judged from the SERR intensities. All immobilization strategies were tested with substrate-bound and free enzyme at different temperatures (4–25 °C) and laser powers (0.5–5 mW). However, in none of the cases could the native P450 state be stabilized.

Electrostatic modulation of the redox potential

The electrochemical response of substrate-free P450 electrostatically adsorbed to negatively coated Ag electrodes was probed by potential-dependent SERR measurements in the range between −0.4 and 0.34 V (Fig. 3).

At all potentials, the SERR spectra of the enzyme immobilized on SAM- and sulfate-coated electrodes could be consistently analyzed on the basis of the four component spectra of the ferric and ferrous 6cLS and 5cHS forms of P420. In this analysis the spectral parameters remain unchanged such that the only variables are the amplitudes of the individual component spectra I_i. These amplitudes are related to the relative concentrations c_i according to

$$c_i = \frac{f_i \cdot I_i}{\sum_i f_i \cdot I_i}, \qquad (1)$$

where the factors f_i are proportional to the relative reciprocal SERR cross sections of the species i. For the

various species of P420, the f_i factors are not known. Therefore, apparent redox potentials E^0_{app} were estimated from fits to the relative intensities I_i (instead of relative concentrations) plotted as a function of the electrode potential (Fig. 4), i.e., setting all the f_i factors equal to1.

The deviation from the true redox potential E^0 depends on the f_{red}/f_{ox} ratio according to

$$E^0 = E^0_{app} + \frac{RT}{zF}\ln\frac{f_{red}}{f_{ox}}, \quad (2)$$

where z is the number of transferred electrons and R, T, and F have the usual meaning. For other heme proteins the f_{red}/f_{ox} ratios have been determined to be between 0.15 and 0.35 [56]. Most likely also for the adsorbed P420 the ratio falls within this range, which would imply that E^0 is more negative by 30–50 mV than the experimentally determined E^0_{app}. The analysis was restricted to the 6cLS redox couples since, except for the sulfate-coated electrode, the reduced 5cHS species was not detectable.

The apparent redox potentials of the 6cLS redox couple display a pronounced variation with the chain length of the SAM (Fig. 5a, Table 2) such that they steadily decrease from 0.21 V (C_{16}) to 0.14 V (C_2).

An even lower value (−0.13 V) was determined for the sulfate-coated electrode. These shifts of E^0_{app} cannot be attributed to the interfacial potential drops, which for negatively charged SAMs on an Ag electrode display the opposite tendency [38]. Instead, taking into account these potential drops, E^0_{app} spans a range from approximately 0.26 (C_{16}) to 0.15 V (C_2).

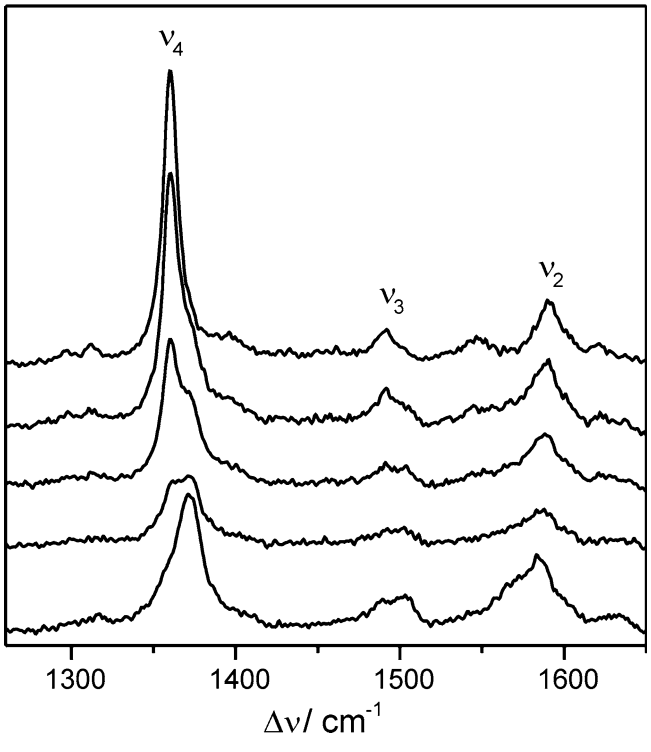

Fig. 3 Selected SERR spectra of P420 immobilized on a mercaptoacetic acid SAM coated electrode recorded as a function of the potential. Potentials from *top to bottom* −0.2, −0.05, 0.05, 0.2, and 0.3 V

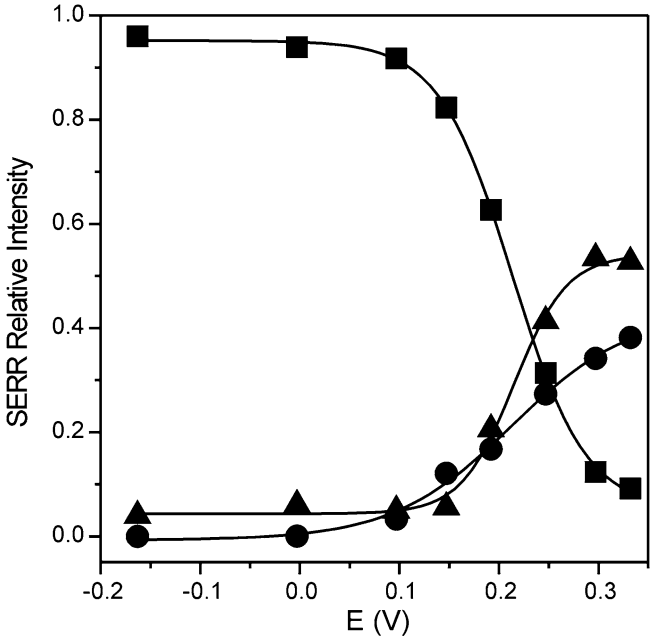

Fig. 4 Relative intensities of the 5cHS and 6cLS species of P420 immobilized on a C_{11} SAM coated electrode, as a function of the potential. *Squares* $6cLS^{red}$, *triangles* $6cLS^{ox}$, *circles* $5cHS^{ox}$

The decrease of the E^0_{app} values on the SAM- and sulfate-coated electrodes seems to be related to the strength of the electric field, which increases upon shortening the chain length. Crucial parameters that control the electric field at the protein binding site are the electrode potential, the SAM length, and particularly the surface charge density σ_C, which for the SAM coatings can be estimated from the pK_a values of the carboxylic head groups according to

$$\sigma_C = \frac{10^{(pH-pK_a)}\sigma_{max}}{1+10^{(pH-pK_a)}}, \quad (3)$$

where $\sigma_{max} = -0.816$ C m^{-2} is the maximum charge density for a fully deprotonated SAM, estimated by geometrical considerations. For the sulfate-coated electrode, an experimentally determined value for σ_C of -0.449 C m^{-2} was adopted from the literature [57]. As shown in Fig. 5b, the apparent redox potentials decrease upon increasing σ_C.

We have previously employed an electrostatic model for the description of the interfacial potential distribution at electrode/SAM/protein interfaces [38]. Within the framework of this model, the electric field strength (E_F) at the surface of the coated electrode is expressed by

$$E_F = \frac{\varepsilon_S \kappa E}{\varepsilon_C + \varepsilon_S \kappa d_C} - \frac{\varepsilon_0 \varepsilon_S \kappa E_{pzc} + \sigma_C}{\varepsilon_0(\varepsilon_C + \varepsilon_S \kappa d_C)}, \quad (4)$$

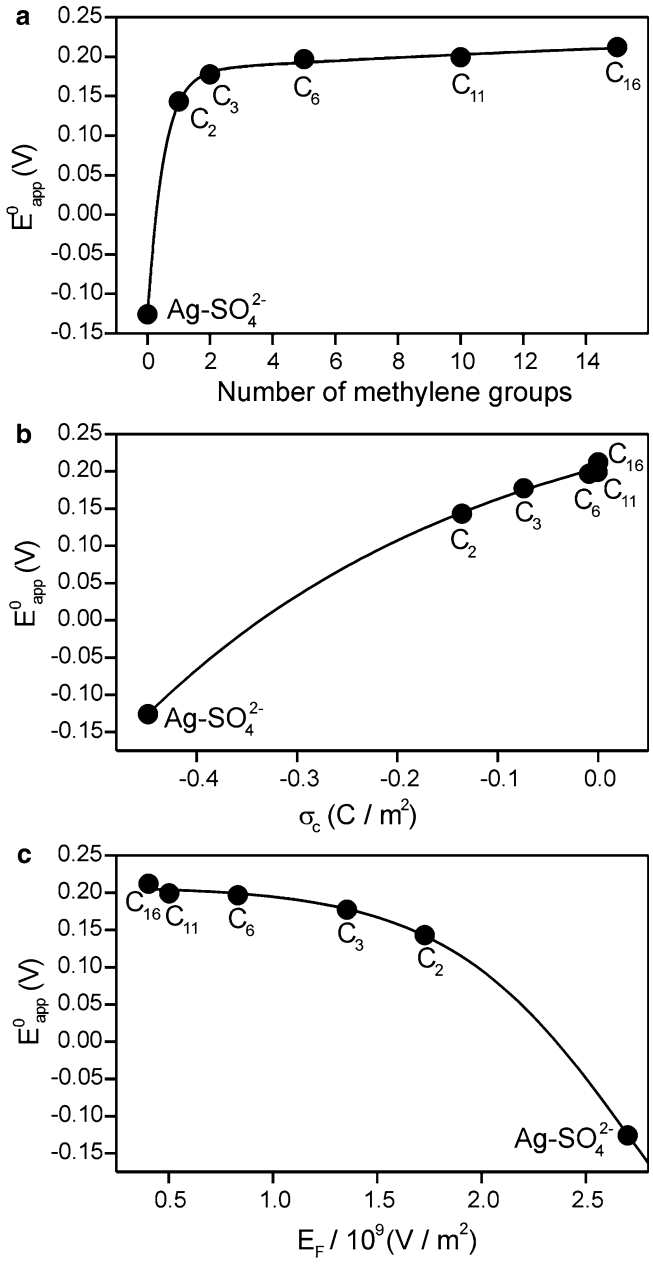

Fig. 5 Variation of the apparent redox potential of electrostatically adsorbed P420 with: **a** chain length of the SAM coating, **b** charge density of the SAM surface, and **c** electric field strength at the SAM surface

where d_C denotes the thickness of the coating, E_{pzc} (−0.773 V) the potential of zero charge, ε_C (2.26) and ε_S (78) the dielectric constants of the SAM and the solvent, respectively, and κ the Debye length. On the basis of Eq. 4, E_F was determined for $E = E^0_{app}$, neglecting the potential-dependent variations of σ_C. The error associated with this approximation does not qualitatively affect the calculations within the potential range and pH values used in the present study.

The data clearly show that the redox potential decreases with increasing electric field strength (Fig. 5c, Table 2), which, hence, is considered to be a crucial determinant for the redox potential of the immobilized enzyme. A recent experimental and theoretical study of cyt-c_3 immobilized on a SAM(C_{11})-coated electrode [40] revealed pronounced electric-field-induced negative shifts of the redox potentials as compared with the protein in solution. Moreover, these shifts are similar to those observed for cyt-c_3 upon complex formation with its natural redox partner. They were rationalized in terms of the stabilization of the ferric state in the local field of the anionic SAM head groups. Accordingly, one would expect the largest negative redox potential shift for P420 on the sulfate-coated electrode and the smallest for the SAM(C_{16})-coated electrode. However, the opposite tendency is observed upon comparing the present data with the redox potential of P420 in solution. For the pressure-induced P420, a redox potential of −0.211 V has been reported [44] that refers to an equilibrium between a dominant 6cLS form and a minor 5cHS species. Thus, the redox potential of the 6cLS form of P420 in solution may be even slightly more negative than −0.211 V taking into account the spin-state dependence of the redox potential of P450 [32]. Hence, there is a positive redox potential shift of at least 0.4 V for the 6cLS form of P420 upon adsorption to SAM(C_{16})-coated electrodes.

Positive shifts of redox potential have generally been observed upon immobilization of P450 to electrodes coated by lipids, detergents, polyelectrolytes, and clays [12–20]. Unfortunately, the electrochemical techniques that have been employed in most of these studies do not provide information about the nature of the electroactive species. Thus, a (partial) conversion to P420 and a shift of the spin equilibrium toward a 5cHS state, which would both correspond to an intrinsic redox potential upshift, cannot be ruled out in each case. However, the redox potentials reported in these studies are generally much more positive than that of P420 in solution, even taking into account a shift of the spin equilibrium toward the 5cHS state. Moreover, it has been shown by measurements in solution that P450 binding to clays [16] or lipids [19] that were employed as coating materials in some of these studies does not induce P420 formation. Specifically for these systems, the electrostatic interactions are likely to be distinctly weaker than for SAMs with carboxylate headgroups. Thus, most likely, the large positive upshift of the redox potential of P420 is not a peculiarity of the electrostatic adsorption on SAM-coated electrodes but appears to be a general phenomenon of immobilization of this enzyme. Since there is no detectable spectral difference between the RR and SERR spectra of P420 in solution and in the immobilized state, major structural changes in the heme pocket such as a ligand exchange are not very likely to be the origin of the potential shift. However, subtle structural changes as well as changes of the surrounding medium may have a substantial impact on the redox potentials of heme proteins [58–69]. An increasing hydrophobicity of the heme environment tends to upshift E^0 owing to stabilization of the formally neutral ferrous form in an

Table 2 Apparent redox potential E^0 for cytochrome P450 (*P450*) and P420 species under different conditions, charge density σ_C, and electric field strength E_F at the surfaces of the electrode coatings as calculated from Eqs. 3 and 4 (see text)

Immobilization conditions	E^0 (V)	σ_C (mC m^{-2})	E_F (V m^{-1}x10^{-9})
Ag/SO_4^{2-}/P420	−0.126[a]	−449	2.84
Ag/C_2/P420	0.143[a]	−136	1.73
Ag/C_3/P420	0.177[a]	−74	1.36
Ag/C_6/P420	0.197[a]	−9	0.83
Ag/C_{11}/P420	0.199[a]	−0.4	0.50
Ag/C_{16}/P420	0.212[a]	−0.03	0.40
P420 (solution)	−0.211[b]	–	–
P450 (substrate free; solution)	−0.303[c]	–	–
P450 (camphor bound; solution)	−0.17[c]	–	–
GCE/clay/P450	−0.139[d]	–	–
PG/DMPC/P450	−0.113[e]	–	–
Au/MPS/PEI/PSS/P450	−0.006[f]	–	–
PG/DDAB/P450	0.006[e]	–	–

[a]This work
[b]From Ref. [44]
[c]From Ref. [59]
[d]From Ref. [16]
[e]From Ref. [19]
[f]From Ref. [17]

environment of low dielectric constant. Likewise, a reduced water accessibility of the heme results in positively shifted E^0 values. Thus, it is possible that in the P420/SAM complex water molecules are removed from the surface binding domain and expelled from the heme pocket. Such effects have not been noted for electron-transferring proteins like cyt-*c* or cyt-c_3, neither upon immobilization to coated electrodes nor in complexes with the respective partner proteins [21, 38, 40]. Thus, the immobilization-induced dehydration may be a specific property of P450. Indeed, the redox potential of P450 shifts up by approximately 0.13 V upon binding of camphor [59], which is known to displace water molecules from the substrate binding site [30]. On the other hand, the redox potentials for P450 on clay-modified electrodes [16] as well as for P420 in solution [44] are insensitive to the addition of camphor, suggesting that the binding site is already dehydrated in both cases. This interpretation may hold as well for P420 on SAM-coated electrodes, which is also insensitive to camphor. However, the large upshifts of the redox potentials observed in the present work with respect to P420 in solution cannot be ascribed to a further dehydration, which, according to Kassner's relation [42, 61], would have a maximum effect of less than 0.2 V. Most likely, the adsorption of the enzyme to negatively coated electrodes leads to a P420 form whose heme environment differs from that of the pressure-induced P420 in solution. Small structural differences, which would be spectroscopically silent, can have a substantial effect on the local electrostatics and therefore on the redox potentials. This interpretation is supported by the fact that the 5cHS/6cLS equilibria are different for the immobilized and the pressured-induced P420 (vide supra).

Whereas immobilization-induced dehydration and alteration of local electrostatics may be the essential origin for the high redox potential of P420 at long SAM lengths, the opposite effect of the electric field strength gains importance with decreasing SAM length, as reflected by the steady decrease of the redox potential. Thus, we conclude that the electric-field dependence of the redox potential of the immobilized P420 reflects the interplay between two opposing effects, the increased hydrophobicity of the heme environment in the SAM/enzyme complex and the destabilization of the ferrous state by the electric field which tend to shift the redox potential to positive and negative values, respectively.

Conclusions

P450 can be efficiently attached to SAM-coated metal electrodes via electrostatic or hydrophobic interactions as well as via covalent cross-linking. In each case, the spectra indicate that the immobilized enzyme is converted to the inactive P420 form which, hence, can be induced by qualitatively different intermolecular interactions. It is very likely that primary adsorption-induced structural changes of the protein may be different for the various monolayers, but in each case they lead to the same changes of the coordination pattern, i.e., the removal or protonation of the thiolate ligand. P420 evidently represents a thermodynamic trap within the conformational space of the protein such that different changes of the protein environment may trigger this conformational transition as is also documented by the various procedures for producing P420 in solution [28, 29, 34, 35, 44, 46–51]. Nevertheless, the substantial discrepancy in the redox potential between the immobilized P420 and the pressure-induced P420 in solution [44] cannot be understood without stressing structural differences in the heme pocket. These differences may refer to the strength of the coordinative bonds of the axial ligands, which appears to be higher at least in the ferrous heme of the immobilized P420 since on SAM-coated electrodes no ferrous 5cHS form is observed in contrast to P420 in solution. The other factors that control the redox potential of the immobilized P420 are ascribed to the dehydration of the enzyme in the protein/SAM interface and the electric-field-induced destabilization of the ferrous state. These factors which affect the redox potential in opposite directions may also be relevant for the P450 state. Thus, the redox potential alone is not a criterion for distinguishing between P450 and P420. An indispensable tool for checking the integrity of the immobilized P450 is the analysis of its active-site structure by spectroscopic techniques such as SERR spectroscopy.

Acknowledgements Financial support by the FCT (POCTI-BIO−43105-2001) and the DFG (Sfb498-A8 and Ju229/4-3) is gratefully acknowledged.

References

1. Danielson PB (2002) Curr Drug Metab 3:561–597
2. Kelly SL, Lamb DC, Jackson CJ, Warrilow AGS, Kelly DE (2003) Adv Microb Physiol 47:131–186
3. Li HY, Poulos TL (2004) Curr Top Med Chem 4:1789–1802
4. Makris TM, Davydov R, Denisov IG, Hoffman BM, Sligar SG (2002) Drug Metab Rev 34:691–708
5. Meunier B, de Visser SP, Shaik S (2004) Chem Rev 104:3947–3980
6. Munro AW, Lindsay JG (1996) Mol Microbiol 20:1115–1125
7. Zangar RC, Davydov DR, Verma S (2004) Toxicol Appl Pharmacol 199:316–331
8. Archakov AI, Ivanov YD (2002) Meth Enzymol 357:94–103
9. Cryle MJ, Stok JE, De Voss JJ (2003) Aust J Chem 56:749–762
10. Guengerich FP (2002) Nat Rev Drug Discov 1:359–366
11. Koeller KM, Wong CH (2001) Nature 409:232–240
12. Davis JJ, Djuricic D, Lo KKW, Wallace ENK, Wong LL, Hill HAO (2000) Faraday Discuss 116:15–22
13. Estavillo C, Lu Z, Jansson I, Schenkman JB, Rusling JF (2003) Biophys Chem 104:291–296
14. Fleming BD, Tian Y, Bell SG, Wong LL, Urlacher V, Hill HAO (2003) Eur J Biochem 270:4082–4088
15. Joseph S, Rusling JF, Lvov YM, Friedberg T, Fuhr U (2003) Biochem Pharmacol 65:1817–1826
16. Lei C, Wollenberger U, Jung C, Scheller F (2000) Biophys Res Commun 268:740–744
17. Lvov YM, Lu ZQ, Schenkman JB, Zu XL, Rusling JF (1998) J Am Chem Soc 120:4073–4080
18. Munge B, Estavillo C, Schenkman JB, Rusling JF (2003) Chembiochem 4:82–89
19. Zhang Z, Nassar AEF, Lu ZQ, Schenkman JB, Rusling JF (1997) J Chem Soc Faraday Trans 93:1769–1774
20. Zu XL, Lu ZQ, Zhang Z, Schenkman JB, Rusling JF (1999) Langmuir 15:7372–7377
21. Murgida DH, Hildebrandt P (2004) Acc Chem Res 37:854–861
22. Macdonald IDG, Smith GCM, Wolf CR, Smith WE (1996) Biochem Biophys Res Comm 226:51–58
23. Quaroni L, Reglinski J, Wolf R, Smith WE (1996) Biochim Biophys Acta 1296:5–8
24. Rospendowski BN, Kelly K, Wolf CR, Smith WE (1991) J Am Chem Soc 113:1217–1225
25. Champion PM, Gunsalus IC, Wagner GC (1978) J Am Chem Soc 100:3743–3751
26. Hudecek J, Anzenbacherova E, Anzenbacher P, Munro AW, Hildebrandt P (2000) Arch Biochem Biophys 383:70–78
27. Jung C (2002) Biophys Acta 1595:309–328
28. Okeefe DH, Ebel RE, Peterson JA, Maxwell JC, Caughey WS (1978) Biochemistry 17:5845–5852
29. Ozaki Y, Kitagawa T, Kyogoku Y, Imai Y, Hashimotoyutsudo C, Sato R (1978) Biochemistry 17:5826–5831
30. Poulos TL, Finzel BC, Howard AJ (1986) Biochemistry 25:5314–5322
31. Shimada H, Nagano S, Ariga Y, Unno M, Egawa T, Hishiki T, Ishimura Y (1999) J Biol Chem 274:9363–9369
32. Sligar SG (1976) Biochemistry 15:5399–5406
33. Stayton PS, Sligar SG (1990) Biochemistry 29:7381–7386
34. Wells AV, Li PS, Champion PM, Martinis SA, Sligar SG (1992) Biochemistry 31:4384–4393
35. Yu CA, Gunsalus IC (1974) J Biol Chem 249:102–106
36. Jung C, Hui Bon Hoa G, Schröder KL, Simon M, Doucet JP (1992) Biochemistry 31:12855–12862
37. Franke A, Stochel G, Jung C, van Eldik R (2004) J Am Chem Soc 126:4181–4191
38. Murgida DH, Hildebrandt P (2001) J Phys Chem B 105:1578–1586
39. Döpner S, Hildebrandt P, Mauk AG, Lenk H, Stempfle W (1996) Spectrochim Acta A Mol Biomol Spectrosc 52:573–584
40. Rivas L, Soares CM, Baptista AM, Simaan J, Di Paolo RE, Murgida DH, Hildebrandt P (2005) Biophys J 88:4188–4199
41. Simaan AJ, Murgida DH, Hildebrandt P (2002) Biopolymers 67:331–334
42. Lewis DFV, Hlavica P (2000) Biochim Biophys Acta 1460:353–374
43. Spiro TG (1985) Adv Prot Chem 37:111–159
44. Martinis SA, Blanke SR, Hager LP, Sligar SG, Hui Bon Hoa G, Rux JJ, Dawson JH (1996) Biochemistry 35:14530–14536
45. Mouro C, Jung C, Bondon A, Simonneaux G (1997) Biochemistry 36:8125–8134
46. Hui Bon Hoa G, Di Primo C, Dondaine I, Sligar SG, Gunsalus IC, Douzou P (1989) Biochemistry 28:651–656
47. Hui Bon Hoa G, Di Primo C, Geze M, Douzou P, Kornblatt JA, Sligar SG (1990) Biochemistry 29:6810–6815
48. Ichikawa Y, Yamano T (1967) Biochim Biophys Acta 147:518–525
49. Ichikawa Y, Yamano T (1967) Biochim Biophys Acta 131:490–497
50. Imai Y, Sato R (1967) Eur J Biochem 1:419–426
51. Omura T, Sato R (1964) J Biol Chem 239:2379–2385
52. Murgida DH, Hildebrandt P (2001) J Am Chem Soc 123:4062–4068
53. Murgida DH, Hildebrandt P (2002) J Phys Chem B 106:12814–12819
54. Oellerich S, Wackerbarth H, Hildebrandt P (2002) J Phys Chem B 106:6566–6580
55. Othman S, Lelirzin A, Desbois A (1994) Biochemistry 33:15437–15448
56. Oellerich S (2001) PhD Thesis, MPI, Germany. ISSN 0932–5131
57. Smolinski S, Zelenay P, Sobkowski J (1998) J Electroanal Chem 442:41–47
58. Barker PD, Nerou EP, Cheesman MR, Thomson AJ, deOliveira P, Hill HAO (1996) Biochemistry 35:13618–13626
59. Fisher MT, Sligar SG (1985) J Am Chem Soc 107:5018–5019
60. Gibney B R, Dutton PL (2001) Adv Inorg Chem 51:295–358
61. Kassner RJ (1973) J Am Chem Soc 95:2674–2677
62. Popovic DM, Zaric SD, Rabenstein B, Knapp EW (2001) J Am Chem Soc 123:6040–6053
63. Rodgers KK, Sligar SG (1991) J Am Chem Soc 113:9419–9421
64. Shifman JM, Gibney BR, Sharp RE, Dutton PL (2000) Biochemistry 39:14813–14821
65. Tezcan FA, Winkler JR, Gray HB (1998) J Am Chem Soc 120:13383–13388
66. Varadarajan R, Zewert TE, Gray HB, Boxer SG (1989) Science 243:69–72
67. Voigt P, Knapp EW (2003) J Biol Chem 278:51993–52001
68. Wirtz M, Oganesyan V, Zhang XJ, Studer J, Rivera M (2000) Faraday Discuss, pp 221–234
69. Wittung-Stafshede P (1999) Biochim Biophys Acta Protein Struct Mol Enzym 1432:401–405